

INELASTIC STRUCTURAL ANALYSIS OF THE MARS TANDEM MIRROR REACTOR

J.P. BLANCHARD and N.M. GHONIEM

Fusion Engineering and Physics Group, University of California, Los Angeles, Los Angeles, CA 90024, USA

Received 13 October 1983

The effects of radiation on the structural performance of fusion reactor structures is recognized as a major issue for the development of fusion reactor technology. Neutron irradiation changes the mechanical properties of structural components resulting in a general degradation of these properties. In addition to the mechanical loads (pressure and weight) and the thermal strains, non-uniform inelastic strain fields are induced by radiation swelling and creep in fusion structures. In this paper, we describe a new computer code, STAIRES, for STress Analysis Including Radiation Effects. This code is based on standard beam theory for pipe-bends. The theory is modified in two areas: (1) consideration of the pipes' cross-section deformation as the radius of curvature changes; and (2) inclusion of inelastic radiation and thermal strains (swelling and creep). An efficient analytical/numerical approach is developed for the solution of indeterminate beam problems. As an application of the method, the stress distribution and deflections of toroidal blanket pipes in the Mirror Advanced Reactor Study (MARS) are evaluated. Swelling strains are identified as a major source of stress and deformation in the proposed blanket design, and possible solutions to the problem are outlined.

1. Introduction

The design of fusion reactor blankets depends critically on the imposed mechanical, thermal and radiation loads. During the past decade, many designs have evolved for blankets that will give maximum nuclear and thermodynamic performance in a given reactor concept. Fusion reactor designers have primarily concentrated on parameters related to the ability of the blanket to absorb neutrons (tritium breeding ratio and energy multiplication factor), and on thermodynamic parameters (pumping power and cycle efficiency). Structural analysis, however, has usually been performed at a crude level to satisfy major failure criteria described by the ASME boiler and pressure vessel code. Radiation effects were included by assigning an arbitrary limit on a given property (usually swelling or loss-of-ductility). With this situation in hand, a great deal of confusion has resulted for estimates of the useful lifetime of fusion reactor structural members. Recently, however, various investigators have attempted to analyze structural aspects of radiation effects in a fusion environment.

Since 1972, a large number of publications have dealt with the problem of estimating the End of Life

(EOL) of fusion structures. Researchers typically used EOL limits on swelling of 2–10% $\Delta v/v$ and uniform elongation of 0.5–2.0% strain [1]. Numerous reviews have been written by Conn [2], Harkness and Cramer [3], and Power and Reich [4]. However, only a few investigators have performed inelastic stress analysis including radiation effects [5–7]. In the analysis of references [5–7] significant restrictive assumptions had to be invoked for the solution of the inelastic problem. For example, Watson [1] developed a 1-D inelastic stress analysis code, TSTRESS, for the calculation of the long-term redistribution of the stresses in a generic thin-walled plate element that is subject to membrane loads. The plate is assumed to be free to expand but is constrained from bending.

A detailed analysis of the time-dependent stresses in a fusion blanket allows the inclusion of more meaningful failure criterion. Mattas [8] and Adegbulugbe and Meyer [9] provide excellent discussions of criterion that are appropriate to designs for which complete structural analyses are available. As these criterion are updated and improved, the reliability of end of life estimates and our confidence in the performance of existing reactor designs will both be increased.

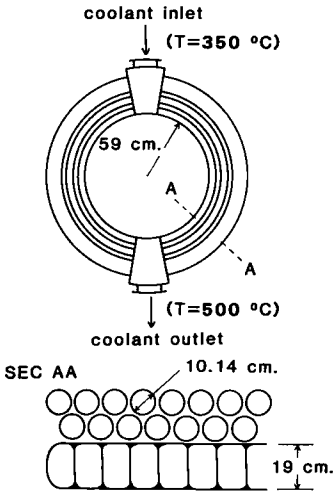


Fig. 1. Cross-section of the MARS blanket.

In this paper a computer code called STAIRE for STress Analysis Including Radiation Effects, is used to calculate the stress and deflection in the coolant pipes of the Mirror Advanced Reactor (MARS) [10] blanket (fig. 1).

The basic design of the blanket is quite simple. The Li-Pb alloy is fed at 350°C to the HT-9 blanket module through a large coolant header at the top. From there, it flows (in parallel) through the rectangular HT-9 beam structure and the 10-cm-diameter circular HT-9 tube section. The tubes in the front ensure uniform flow in the regions where the neutron heating is the highest, and the rectangular sections are better suited to attain a low void fraction to increase the neutron energy multiplication factor. The LiPb exits at 500°C through a large-diameter coolant pipe to a double-walled heat exchanger. The larger pipes are necessary to reduce the MHD pumping power losses.

The STAIRE code uses virtual work principles to simultaneously determine the reactions and deflections for beams of arbitrary cross-section. This classical beam theory is modified to account for the increased flexibility of hollow, curved beams during bending [11]. After completing this structural analysis, end-of-life criteria such as stress or deformation limits are incorporated to determine the blanket lifetime. In order to account for uncertainties in modeling or material constants, probabilistic methods are used to determine failure frequencies, thus providing an indication of the MARS blanket reliability.

2. Theory

The analysis begins with the determination of the redundant end reactions which result from the applied strains. Fig. 2 shows the configuration of the pipe model used to approximate the MARS blanket. XM, XF and XP are unknown end reactions, θ denotes position along the pipe and ξ , the distance from the neutral axis, denotes position on the cross-section.

Because the tube is curved and statically indeterminate, we are unable to separate the axial problem from the radial and rotational problems. Using virtual work principles, it is possible to develop the flexibility matrix for the pipe [12]. This matrix gives the deflections at the free (cut) end of a singly clamped pipe due to unit loads at that end,

$$\mathbf{F} = \begin{bmatrix} f_{MM} & f_{MF} & f_{MP} \\ f_{FM} & f_{FF} & f_{FP} \\ f_{PM} & f_{PF} & f_{PP} \end{bmatrix} = \frac{1}{EI} \begin{bmatrix} \int dx & \int y ds & \int x ds \\ \int y ds & \int y^2 ds & \int xy ds \\ \int x ds & \int xy ds & \int x^2 ds \end{bmatrix}; \quad (1)$$

where the first row of the matrix equation gives the rotations due to unit moment, unit axial force and unit radial force, going from left to right. The second row will similarly give the axial deflections and the third row gives the radial deflections due to unit loads at

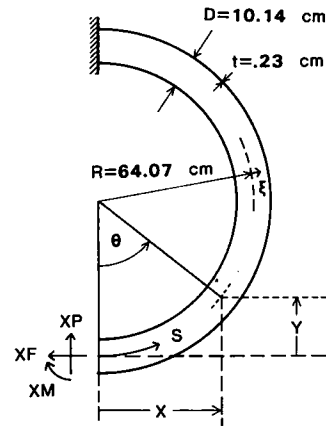


Fig. 2. Model geometry for analysis of the coolant tubes.

the cut. E is the modulus of elasticity and I is the moment of inertia of the cross-section.

The matrix, F , is used to form an equation for the rotation and axial and radial deflections of the free end of the pipe due to both the end forces and applied strains. The end deflections due to end forces are FX where X is a vector of unknown end reactions:

$$X = \begin{bmatrix} X_M \\ X_F \\ X_P \end{bmatrix}. \quad (2)$$

If we add the deflections due to the input strains given by a vector E , to the deflections due to end forces, we obtain a vector, D , containing the resultant end rotation and deflection. The final equation becomes

$$FX + E = D. \quad (3)$$

The vector D is generally determined by the boundary conditions. For example, if both ends of the pipe are clamped, there are no end rotations or deflections and D is identically zero. Prescribed end translations or rotations can also be included here.

Assuming F , E and D are known, the unknown reactions are easily found by solving the matrix equation (3) for the vector X . The result is $X = F^{-1}[D - E]$. In the following, we describe a method for determination of the vector E from input thermal and radiation strains.

The general form of E is shown by reference [12] to be of the form:

$$E = - \begin{bmatrix} \int w' ds \\ \int w'y ds - \int \bar{e}' \cos \theta ds \\ \int w'x ds + \int \bar{e}' \sin \theta ds \end{bmatrix}, \quad (4)$$

where w' is the change in curvature due to inelastic strains and \bar{e}' is the average inelastic strain at a given cross section. The average strain can be found easily, $\bar{e}' = (1/A) \int e' dA$, but w' requires additional information. Assuming that yielding does not occur, e' becomes the total inelastic strain due to thermal expansion, αT , swelling, $\Delta v/3v$, irradiation creep, e'_{irr} , and thermal creep, e'_{th} :

$$e' = \alpha T + \frac{\Delta v}{3v} + \epsilon'_{irr} + \epsilon'_{th}. \quad (5)$$

To determine the change of curvature under loading conditions, we begin with a strain-curvature rela-

tion. In standard beam theory the strain is given as:

$$e = -\xi w. \quad (6)$$

This equation is valid if the beam's cross section remains unchanged during deformation, but in our case of a thin-walled, curved tube, it requires modification. Hovgaard [11] postulates the following:

$$e = -\xi w - \Delta\xi/R_c, \quad (7)$$

where $\Delta\xi$ is the radial displacement of a point on the tube relative to the neutral axis. The shape of the final cross-section is nearly elliptical. Hovgaard found:

$$\Delta\xi = -K_1 \xi^3 R_c w, \quad (8)$$

where K_1 is a constant determined by the pipe geometry:

$$K_1 = 6r^2/(6t^2 R_c^2 + 5r^4), \quad (9)$$

where r is the pipe radius, t is the pipe wall thickness, and R_c is the distance from the plasma center to the pipe's central axis. This relation for $\Delta\xi$ leads to a near-elliptical cross section during bending.

Plugging the $\Delta\xi$ relation into eq. (7), gives:

$$e = -(1 - K_1 \xi^2) \xi w. \quad (10)$$

For a given curvature change (w), the strain away from the neutral axis is less than beam theory predicts. This leads to stress relaxation at the outer fibers and an increased pipe flexibility because more rotation is required to provide equilibrium for a given force at any cross section. In our case, the "loads" are input strains, rather than applied forces, so the increased pipe flexibility leads to smaller reactions resulting from the given strains. The stresses in the pipe are therefore less than the standard beam theory would predict.

In order to find the curvature as a function of inputs only, we next require a constitutive relation. Assuming that the total strain can be separated into elastic and inelastic portions, the constitutive equation is given by

$$e = \sigma/E + e', \quad (11)$$

where e is the total strain and σ/E is the elastic strain. Substituting into the strain-curvature relation Eq. (10), multiplying by $(\xi - \Delta\xi)$ and integrating over the cross-section we obtain,

$$\int \frac{\sigma}{E} (\xi - \Delta\xi) dA + \int e' (\xi - \Delta\xi) dA = -w \int (\xi - \Delta\xi) (1 - K_1 \xi^2) \xi dA. \quad (12)$$

The applied moment, M , on any cross section is given by $M = \int \sigma(\xi - \Delta\xi) dA$. Using this fact and ignoring second order terms, we can solve for w :

$$w = \frac{-M}{K_{III}E} - \frac{1}{K_{III}} \int e' \xi dA, \quad (13)$$

where

$$K_{III} = K_{II}I + K_I R_c \int e' \xi^3 dA, \quad (14)$$

and

$$K_{II} = \frac{12I^2 R_c^2 + r^4}{12I^2 R_c^2 + 10r^4}. \quad (15)$$

The constant K_{II} effectively reduces the pipe's moment of inertia, accounting for much of the pipe's increased flexibility. Since w' is the change in curvature due only to the inelastic strains, it is found by setting the applied moment equal to zero: $w' = -(1/K_{III}) \int e' \xi dA$. This completes the requirements for the determination of the redundant reaction vector \mathbf{X} .

Now that the end reactions are known, the axial stresses in the pipe can be found. The first step is to find the resultant forces and moment acting on any cross section of the pipe using simple statics.

$$M = X_M + xX_P + yX_F, \quad (16)$$

$$F = X_F \cos \theta - X_P \sin \theta, \quad (17)$$

$$P = X_F \sin \theta + X_P \cos \theta, \quad (18)$$

where M , F and P are the moment and forces on a section at an angle θ .

In determining the stresses, we must modify the constitutive equation to allow for a strain, e_0 , at the neutral axis. This strain has no effect on the determination of w , but it is significant here. By integrating the new constitutive equation, $e = e' + \sigma/E + e_0$, over the area and using $F = \int \sigma dA$, we obtain an equation for e_0 :

$$e_0 = \frac{-F}{AE} - \frac{1}{A} \int e' dA, \quad (19)$$

we now have,

$$\frac{\sigma}{E} = e - e' + \bar{e} + \frac{F}{AE}. \quad (20)$$

Substituting for both w and e yields the final result:

$$\sigma_{axial} = \frac{F}{A} + \xi(1 - K_I \xi^2) \left(\frac{M}{K_{III}} - Ew' \right) - E(e' - \bar{e}). \quad (21)$$

Our last goal is to find the deflections as a function of toroidal angle. The process followed is similar to determination of the end reactions. The deflections are found by conceptually cutting the pipe at the angle θ and using the equation, $\mathbf{FX} + \mathbf{E} = \mathbf{D}$. In this case, \mathbf{D} is unknown and \mathbf{FX} and \mathbf{E} must be determined. \mathbf{F} and \mathbf{E} are as given before, except any integrals must be performed only from the cut to the pipe end and the origin of x and y is always at the cut with x tangential to the pipe. The vector \mathbf{X} is now filled with the forces at $\theta = \theta$, M , F and P . \mathbf{D} then gives us the deflection at the cut.

We must still describe the nature of e' . For thermal strains, we have $e_{th} = \alpha T$ where α is the thermal expansion coefficient and T is the difference between the operating temperature and the zero stress temperature. For the swelling strains, e^s , we use a design equation developed by Ghoniem and Conn for ferritic alloys [13]:

$$e^s = \frac{1}{3} \frac{\Delta v}{v} = \frac{1}{300} \exp \left\{ \left(\frac{T - T_p}{\gamma} \right)^2 \right\} \times \{0.036\delta - 0.074\} \{ \phi(C_r) \}, \quad (22)$$

where

$$\begin{aligned} T_p &= \text{the peak swelling temperature (}^\circ\text{C)} = 425^\circ\text{C} \\ &\quad \text{for HT-9,} \\ \gamma &= \text{the Gaussian width} = 59(^\circ\text{C}), \\ \delta &= \text{displacement dose (dpa),} \end{aligned}$$

$$\phi(C_r) = \begin{cases} 0.067 C_r^2 - 0.457 C_r + 1.0 & \text{for } C_r < 5\% , \\ 0.037 C_r + 0.237 & \text{for } C_r > 5\% , \end{cases} \quad (24)$$

and C_r is the chromium content, in percent.

Irradiation creep data exists for a limited number of ferritic alloys. Odette [14] compiled such information, with a suggested correlation of the form:

$$\dot{e}_{irr}^c = A_c \sigma \delta, \quad (24)$$

where A_c is a constant, σ the applied Von Mises (equivalent) stress, and δ is the irradiation dose. The values of A_c seem to be both temperature and alloy dependent. Values ranging from $1 \times 10^{-7} \text{ dpa}^{-1} \text{ MPa}^{-1}$ to $2.9 \times 10^{-6} \text{ dpa}^{-1} \text{ MPa}^{-1}$ were reported.

The following equation, developed by Amodeo and Ghoniem [15], is used for thermal creep:

$$e_{th}^c = \frac{2.26 \times 10^{-5}}{KT} \exp \left(-\frac{1.23}{KT} \right) (\sigma - \sigma_0)^3, \quad (25)$$

and

$$\sigma_0 = 1366.4 - 1.51 T \text{ (MPa)}, \quad (26)$$

where T is the absolute temperature and σ_0 is the temperature dependent back stress. Our analysis requirements are now complete.

3. Stresses due to swelling

Because swelling induced volume increases of a few percent cause very large stresses when creep strains are not accounted for, the results presented in this section will not consider plasticity effects. It will be seen in later sections that irradiation creep reduces the stresses in the blanket to values well below the yield stress of HT-9.

Fig. 3 shows the axial stresses along the pipe for a uniform damage rate of 69 dpa/yr. Thermal stresses right after startup are quite small, but the maximum stress increases rapidly as swelling occurs. The non-symmetric distribution is due to the highly non-linear temperature dependence of the void growth.

One result of the tube's cross-section deformation is an altered stress distribution over the cross-section. A rigid cross-section would experience a linear stress dependence as a function of ξ , but in fig. 4 we see a parabolic distribution for the curved, hollow tube. The stresses at the extreme fibers are smaller than one might normally predict because of the tube's increased flexibility.

In addition to the stress levels in a blanket, designers must also consider the pipe deflections. Fig. 5 shows that the maximum radial deflection is about 0.5 cm after startup and increased by another 0.5 cm/yr thereafter. These deflections are not severe and should cause no significant design problems.

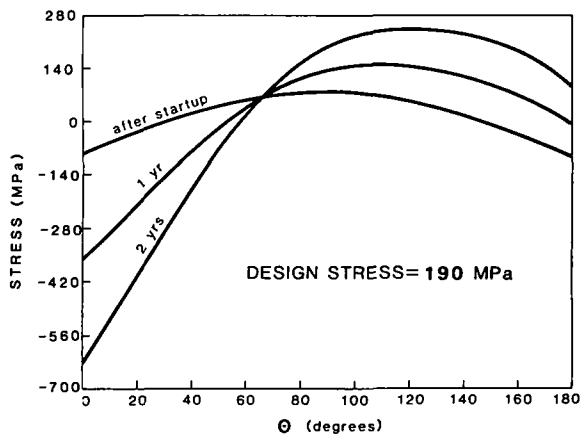


Fig. 3. Axial stresses at $\xi = 4.3$ cm for clamped pipe.

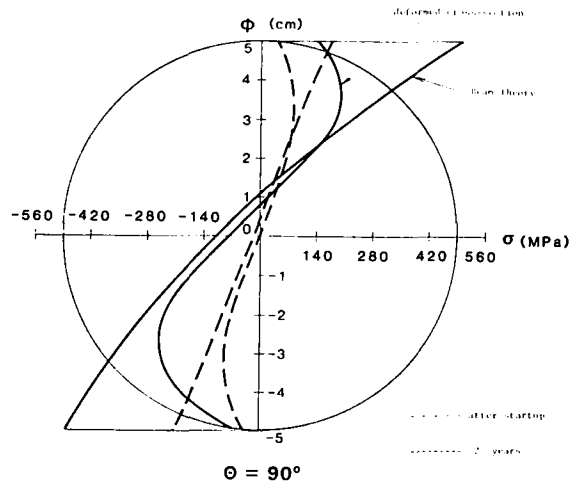


Fig. 4. Stress distribution over cross-section.

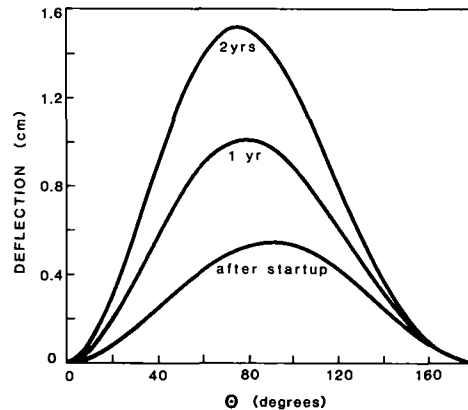


Fig. 5. Radial deflections for clamped pipe.

4. Possible design modification

In order to reduce the somewhat threatening stress levels caused by swelling, the blanket design could be altered to better accommodate the swelling. Smaller stresses would provide greater margin with the design stress and decrease the creep strains, which would lead to rupture. Additionally, the design would not be forced to rely on creep alone to provide adequately low stresses. This is desirable because the sparse data for the creep of HT-9 leads to great uncertainty in the amount of stress relief due to creep.

In this blanket, the simplest way to accommodate swelling is to allow the pipe headers to translate

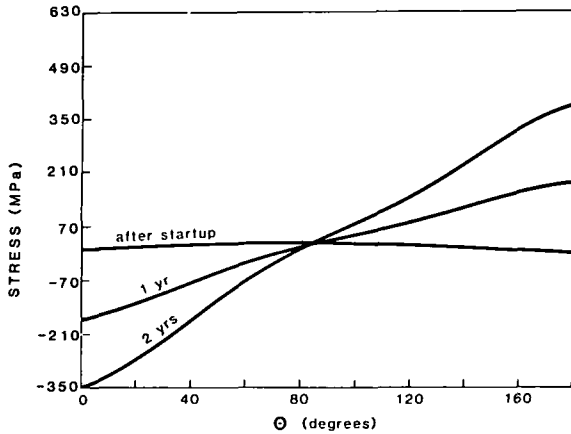


Fig. 6. Axial stresses assuming free header translation.

radially. In order to approximate free translation, the headers are assumed to translate 0.25 cm/yr; the stresses are given in fig. 6. The stresses after startup are nearly zero, but the non-symmetric swelling distribution cannot be completely accommodated. Nevertheless, the maximum stresses are nearly halved. The question of tensile behavior vs. compressive behavior is not important here because the stresses are roughly symmetric about the neutral axis, as seen in fig. 4. Therefore, a compressive stress in fig. 6 will correspond to a tensile stress of similar magnitude on the opposite side of the neutral axis.

5. Influence of irradiation creep

Because the MARS design features indeterminate structures with no applied loads, creep leads to lower stresses rather than increased total strains as one would normally expect. Because swelling constantly tries to increase the stresses, one can envision the pipe reaching a steady-state in which the stress increase due to swelling is balanced by the decrease due to creep. In fig. 7, the maximum stress history is shown for swelling alone and for one value of A_c . The steady state stress is determined by the creep-free elastic strain rate divided by the creep coefficient.

Contrary to what one might expect, the pipe deflections do not change when creep is included, i.e., the pipe expands with time as if the creep coefficient is zero. This can be understood by more closely investigating the distribution of creep strains over the cross-section. Because creep is proportional to the

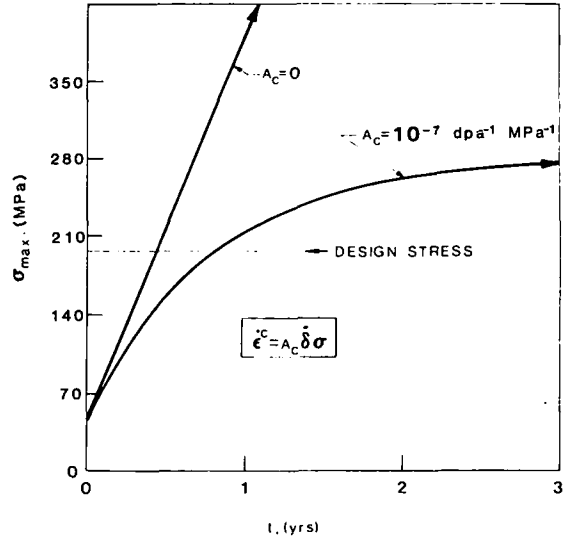


Fig. 7. Maximum stress history with and without irradiation creep.

local stress and the stress is an odd function over the cross-section, the creep strains are negative on the inner fibers ($\xi < 0$) and positive on the outer fibers ($\xi > 0$). As a result, the pipe accommodates creep by decreasing the elastic strains rather than increasing the total strains. In terms of our model, the radial deflections of the clamped pipe are caused by $\bar{\epsilon}'$ alone and the creep strains do not contribute significantly to this quantity.

6. Damage gradient effects

The previous analysis has been performed under the assumption that the damage rate (69 dpa/yr) was uniform everywhere in the pipe. In reality, 3-D neutronics Monte Carlo calculations in the MARS study found that the damage rate at the back of the pipe is about half that at the front [10]. This affects the results in two ways. First, the swelling is taken to be a linear function of the dose, so it decreases with major radius. Second, the irradiation creep shows similar behavior, because it is proportional to the dose rate.

Fig. 8 exhibits the deleterious effects of a damage gradient on the stress distribution in the pipe. Although the overall damage in the pipe has decreased, the maximum stress actually increases due to the overall decrease in the creep coefficient. Fortunately, the stress at the welds ($\theta = 0$), which will likely be the pipes' weakest points, decreases by a small amount.

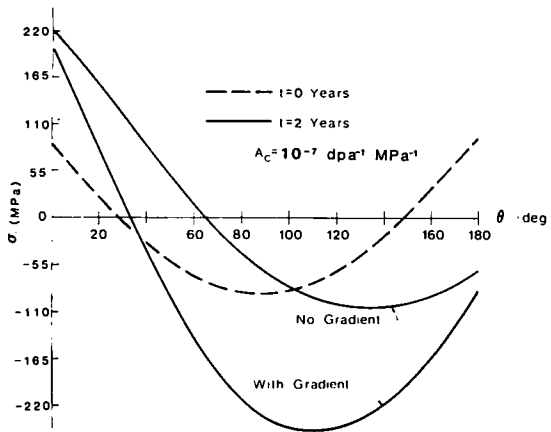


Fig. 8. Stress distribution in clamped pipe with and without damage gradient.

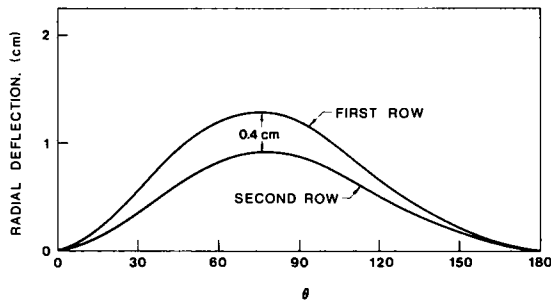


Fig. 9. Radial deflections after two years.

The gradient also affects the blanket design through differential expansion between the first and second rows of tubes. In fig. 9 we see that after two full power years, the maximum radial deflection is about 1.3 cm in the first tube bank and 0.9 cm in the second bank. Therefore, a 0.4 cm gap would be required in the initial design to prevent tube/tube interaction. A larger initial gap would be required for a longer expected lifetime.

7. Thermal creep

From the available HT-9 data, it appears that at temperatures near or below 500°C, thermal creep can be neglected if the stress levels are below about 280 MPa. Because the structure temperatures in the MARS blanket are limited to about 530°C by the compatibility of the LiPb coolant with HT-9 and the

stresses are maintained below 280 MPa (as seen in fig. 7), the previous analyses will not be substantially affected by thermal creep.

In order to assess the structural response to the temperature and non-linear stress dependencies of thermal creep, we will consider an illustrative case in which the inlet and outlet coolant temperatures will be 450°C and 550°C, respectively. Irradiation creep will be neglected in this temperature range, so that the effects of thermal creep will be isolated. The assumed coolant temperatures might be seen in a blanket for which the designer attempts to avoid the ductile-to-brittle transition temperature (DBTT) of HT-9 and keep the structure temperature away from the peak swelling temperature of 425°C.

The effect of thermal creep on the stress distribution in the pipe is shown in fig. 10. The stress is redistributed by the deformation, increasing in some places and decreasing in others. This non-uniform effect results from the temperature dependence and non-linear stress dependence of the creep law. In the case of irradiation creep, the creep rate is linear in the stress and is unaffected by temperature over the range used, so the relaxation process occurs uniformly and the shape of the stress distribution is unchanged.

Although thermal creep appears to have increased the blanket lifetime by decreasing the stresses at the welds, the increased deformation due to creep strains must also be considered as a cause of failure. If we impose a limit of one percent on the accumulated creep strains (as seen in the ASME Boiler and Pressure Vessel code), the life would be limited to less than three years by thermal creep alone. A limit of one percent on the total permanent strain would decrease the lifetime to below two years and the

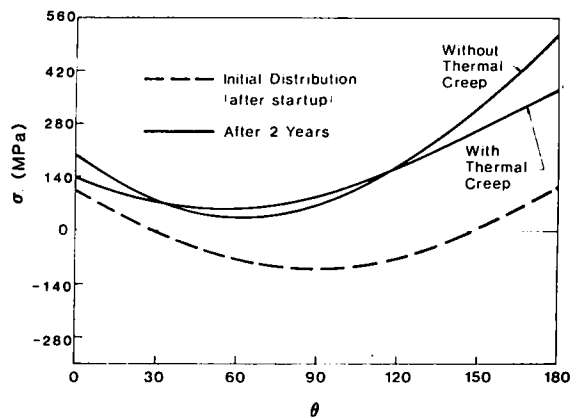


Fig. 10. Effect of thermal creep on stress distribution.

inclusion of irradiation creep would further increase the permanent strain. Apparently, operating the blanket in this high temperature range is not beneficial because of the high creep rates.

8. Lifetime prediction

Because of the uncertainties in the material properties and modelling of any structural analysis, the most realistic result is a frequency of failure, rather than an absolute failure time. In the context of this paper, we will illustrate this method by focusing on irradiation creep, predicting the failure frequency using an assumed probability of occurrence for the creep compliance, A_c . The EOL criterion will vary, depending on the extent of the analysis.

In fig. 11, the EOL is shown for a design stress limit of 190 MPa at 500°C [16] and two different strain limits. Apparently, the lifetime will be primarily strain limited and the failure will occur by loss of structural integrity or rupture.

In order to determine the frequency of failure, we will use the more conservative limit of 2% permanent strain and assume that A_c has an equal probability of occurrence anywhere in the measured range of the available data [14] and no probability outside that range. A more realistic assumption might be some type of normal distribution, but a uniform occurrence will be adequate for demonstration purposes. Fig. 12 shows that, under the assumed operating conditions, over 90% of the coolant pipes in the MARS blanket should survive nearly three years. The abrupt change in the predicted frequency at about 2.8 years is due to

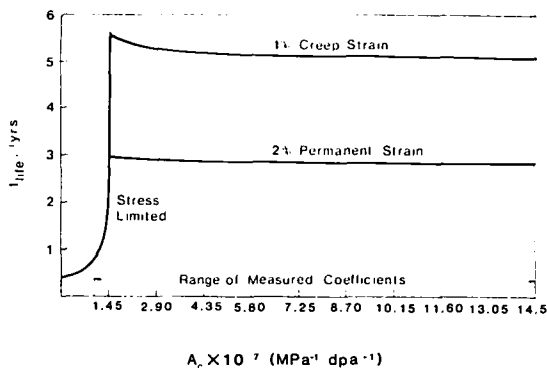


Fig. 11. Blanket lifetime as function of creep coefficient.

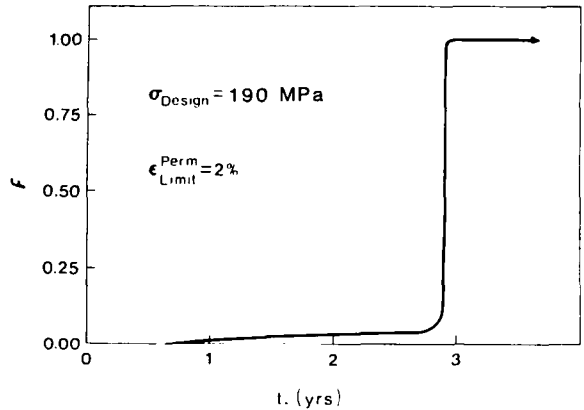


Fig. 12. Failure frequency for uniform distribution of A_c .

the fact that the vast majority of the pipes will be in the strain limited region, where the EOL is nearly independent of A_c . If the less conservative (and perhaps more realistic) EOL criterion of 1% creep is used, a life of nearly five years could be expected for the majority of the pipes. Hopefully, this will be more than adequate for an economical reactor concept.

9. Summary and conclusions

Despite the relatively large damage rates in the MARS blanket, it appears that proper design and sufficient relief by creep will allow the stresses to remain below proposed limits indefinitely. Unfortunately, this does not ensure infinite life because limits must be imposed on creep strains in order to prevent failure by creep rupture. Even with conservative limits imposed on the total creep deformation, the blanket is estimated to have a lifetime of 3–5 years for the expected operating conditions.

Although a lifetime of a few years is in the vicinity of what one might expect, the many uncertainties inherent in the expected failure modes and adopted criterion reduce confidence in present estimates. Specifically, data shortages have forced us to treat creep rupture rather simplistically and completely neglect stress-corrosion cracking and creep crack growth as possible failure modes. The analytical tools presented here are sufficient for a reliable lifetime estimate, but a better understanding of the nature of the blanket failure must first be obtained.

Acknowledgment

This work is supported by the US Department of Energy under contract DE-AM03-76SF00034 P.A. #DE-AT03-82ER52084 with UCLA.

References

- [1] R.D. Watson, The impact of inelastic deformation, radiation effects, and fatigue damage on fusion reactor first wall lifetime, Ph.D. Thesis, University of Wisconsin, Madison, WI (December 1981) p. 26.
- [2] R.W. Conn, First wall and divertor plate material selection in fusion reactors, University of Wisconsin, Report, UWFD-237 (1978).
- [3] S.D. Harkness and B.A. Cramer, Review of lifetime analysis for tokamaks, *J. Nucl. Mater.* 85 & 86 (1979) 135.
- [4] J.R. Power and M. Reich, A review of structure mechanics aspects of fusion blankets, *Nucl. Engrg. Des.* 58 (1980) 247.
- [5] B.M. Ma, Irradiation swelling, creep, thermal shock and thermal cycling fatigue analysis of cylindrical controlled thermonuclear reactor first wall, *Nucl. Engrg. Des.* 28 (1974) 1.
- [6] W. Daenner and J. Raeder, Latest results from the FWLTB computer code: the influence of a fusion reactor, *J. Nucl. Mater.* 85 & 86 (1979) 147.
- [7] R.D. Watson, R.R. Peterson and W.G. Wolfer, The effect of irradiation creep, swelling, wall erosion and embrittlement on the fatigue life of a tokamak first wall, University of Wisconsin Report, UWFD-433 (August 1981).
- [8] R.F. Mattas, Fusion component lifetime analysis, ANL/FPP/TM-160 (1980).
- [9] A.O. Adegbulugbe and J.E. Meyer, Failure criteria for fusion reactor first wall structural design, *J. Nucl. Mater.* 103 & 104 (1981) 161.
- [10] B.G. Logan et al., Mirror advanced reactor study interim design report, Lawrence Livermore National Laboratory Report, UCRL-53333 (April, 1983).
- [11] W. Hovgaard, The elastic deformation of pipe-bends, *J. Maths. and Physics* 5-6 (1925-1927) 69.
- [12] Republic Aviation Corp., Thermo-structural Analysis Manual (Farmingdale, New York, 1964).
- [13] N.M. Ghoniem and R.W. Conn, Assessment of ferritic steels for steady-state fusion reactors, IAEA Technical Committee Meeting and Workshop on Fusion Reactor Design and Technology, Tokyo, Japan, October 5-16, 1981.
- [14] G.R. Odette, Property correlations for ferritic steels for fusion applications, Damage Analysis and Fundamental Studies Information Meeting, October 2-3, 1980.
- [15] R.J. Amodeo and N.M. Ghoniem, Constitutive design equations for thermal creep deformation of HT-9, *Nucl. Engrg. Des./Fusion* 2 (1984).
- [16] N.M. Ghoniem, J. Blink and N. Hoffman, Selection of alloy steel type for fusion power plant applications in the 350-500°C range, Proc. of the Topical Conf. on Ferritic Alloys for Use in Nuclear Technology, Snowbird, Utah, 1983.